CONFERENCE PRE-PRINT

OVERVIEW OF THE DESIGN AND PROCUREMENT OF ECRH SYSTEM FOR DTT

S. GARAVAGLIA
Istituto per la Scienza e la Tecnologia dei Plasmi, CNR
Milano, Italy
Email: saul.garavaglia@istp.cnr.it

A. ROMANO
DTT S.C. a r.l.,
Frascati (RM), Italy
and
ENEA, Fusion and Nuclear Safety Department, C.R. Frascati,
Frascati (RM), Italy

G. GRANUCCI
Istituto per la Scienza e la Tecnologia dei Plasmi, CNR
Milano, Italy
and
DTT S.C. a r.l.
Frascati (RM), Italy

S. BERTOLAMI, F. DI PAOLO
University of Rome Tor Vergata, Department of Electronics Engineering
Roma, Italy

M. BONESSO, R. DIMA, A. PEPATO, P. REBESAN, M. TURCATO
National Institute for Nuclear Physics (INFN)
Padova, Italy

A. BRUSCHI, B. BAIOCCHI, F. FANALE, L. FIGINI, A. MORO, P. PLATANIA, N. RISPOLI, A. SIMONETTO
Istituto per la Scienza e la Tecnologia dei Plasmi, CNR
Milano, Italy

D.BUSI, A. PAGLIARO
Department of Mechanical Engineering, Politecnico di Milano
Milano, Italy

A. CALAMIDA
ENEA, Fusion and Nuclear Safety Department, C.R. Frascati,
Frascati, Italy

M. DE NARDI, A. MAISTRELLO
Consorzio RFX (CNR, ENEA, INFN, University of Padova, Acciaierie Venete SpA)
Padova, Italy

P. FANELLI
Department of Economy, Engineering, Society and Business (DEIM), University of Tuscia
Viterbo, Italy

D. CESTER, G. FAVERO
National Institute for Nuclear Physics (INFN)
Padova, Italy
and
Department of Management and Engineering, University of Padova

Padova, Vicenza, Italy

E. GAJETTI, L. SAVOLDI
MAHTEP Group, Dipartimento Energia "Galileo Ferraris", Politecnico di Torino
Torino, Italy

M. RECCHIA
Consorzio RFX (CNR, ENEA, INFN, University of Padova, Acciaierie Venete SpA)
Padova, Italy
and
Istituto per la Scienza e la Tecnologia dei Plasmi, CNR
Padova, Italy

A. SALVITTI
DTT S.C. a r.l.,
Frascati (RM), Italy

DTT CONTRIBUTORS
DTT S.C. a r.l.
Frascati (RM), Italy

Abstract

The Divertor Tokamak Test facility is being developed to address the critical challenge of power exhaust in preparation for the DEMO fusion power plant. Central to this effort is the installation of one of the largest ECRH systems, which will be implemented in two phases: 16 gyrotrons in the first stage (14.4 MW at plasma), expanding to 32 units (28.8 MW or more) at later stages. The system is arranged into four clusters, each comprising eight gyrotrons with associated power supplies, connected via a quasi-optical evacuated Transmission Line (TL) and two launchers installed in the vacuum vessel. The ECRH system will provide localized heating and current drive, as well as advanced plasma control functions such as stabilization of neoclassical tearing modes. Launcher design studies addressed structural stresses caused by induced currents during major disruptions and vertical displacement events, particularly in high-field regions. Proposed solutions include minimizing horizontal extensions, adopting cage-type structures, and optimizing mirror design to reduce electromagnetic and thermal loads. For the TL, the conceptual design is completed and mirror prototyping is underway using additive manufacturing techniques. Analyses confirmed target transmission efficiencies above 90% under ideal conditions, while non-idealities such as surface deformation were shown to increase stray radiation. For extremely loaded mirrors, like polarizers, efficient cooling solutions based on triply-periodic minimal surfaces were investigated. The gyrotrons, supplied by Thales under a joint procurement with F4E, are based on the design of a prototype developed in view of ITER designs, each delivering 1 MW at 170 GHz for 100 s with >40% efficiency. The first unit has been tested successfully, and production of the next 15 is underway. High-Voltage Power Supplies provide fast dynamics to stabilize RF output and suppress unwanted modes. Finally, the control system integrates all subsystems through standardized Plant System Units, ensuring uniform operation and safe coordination between the ECRH plant, CODAS, and Plasma Control System.

1. INTRODUCTION

The Divertor Tokamak Test (DTT) facility [1] is under construction with the objective of developing solutions for power exhaust, a key challenge for the design of the future fusion power plant DEMO. DTT is a D-shaped superconducting tokamak ($B_T \leq 5.85$ T, $I_P \leq 5.5$ MA, $R_0 = 2.19$ m, $a = 0.7$ m) capable of pulses up to 100 s with a repetition rate of one pulse per hour. Both the first wall and divertor are made of tungsten. The device will employ up to 45 MW of auxiliary heating power to reproduce the target DEMO exhaust load ($P_{SEP}/R = 15$ MW/m) on the divertor. To achieve this, DTT will host one of the world's largest ECRH systems, whose installed power will grow in two main stages in line with the machine development program. In the initial phase, 16 units will deliver 14.4 MW to the plasma. This will be doubled in the third DTT phase, with further 16 units to reach a total of 28.8 MW at plasma or potentially more if higher-power units become available with a target efficiency >90%. The schedule is based on the development of an ECRH system structured in four clusters, each consisting of 8 gyrotrons and related Power Supplies (PS), located in a building 80 m from the tokamak hall. These 8 sources are connected to the DTT tokamak through a single/multi-beam evacuated Quasi-Optical (QO) Transmission Line (TL) installed on a bridge (connecting the tokamak hall with the gyrotron building) and two launching antennas positioned in the equatorial and upper ports of the same vacuum vessel sector [2, 3]. The system is primarily designed for main plasma heating while its high flexibility also supports various functions throughout the plasma pulse, such as the stabilization of Neoclassical Tearing Modes (NTM), as outlined in [4]. Dedicated studies have been performed regarding the EC beam characterization aimed at verifying the fulfilment of the tasks foreseen for the different operational phases of the machine and during the various phases of the discharges. Studies have been carried out in order to assess the EC stray radiation to calculate the possible load on the first wall due to unabsorbed RF power when impacting diagnostics.

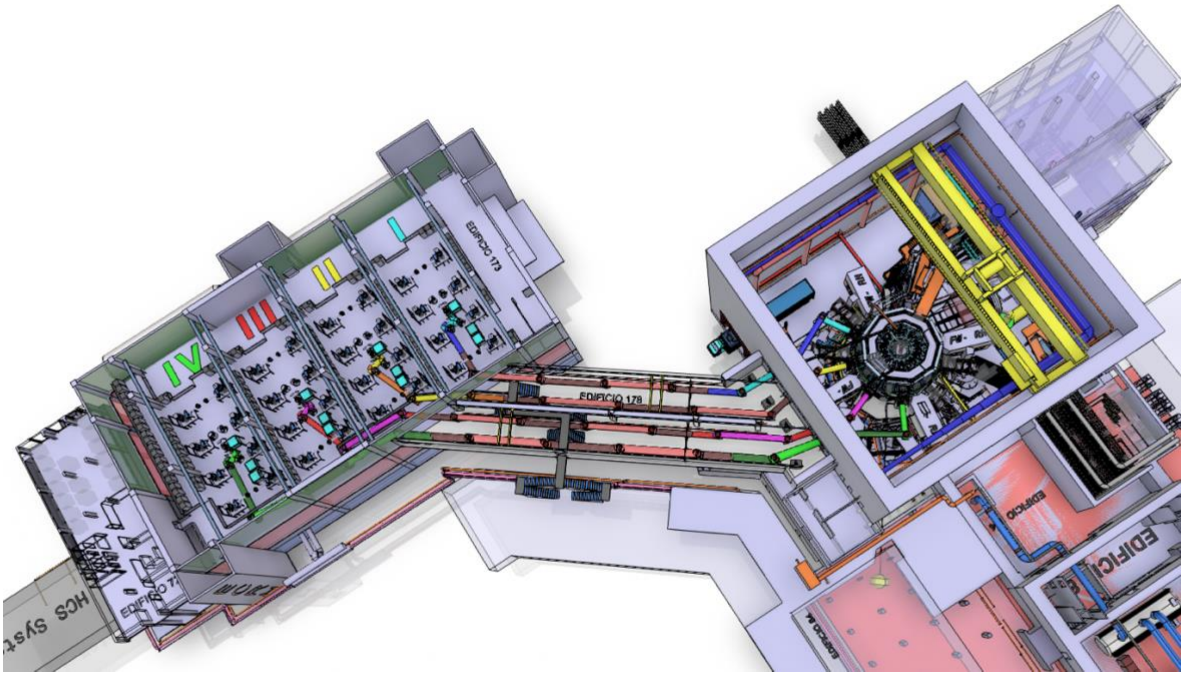

FIG. 1. Top view of the ECRH system. The ECRH building (left) and the tokamak hall building (right) are joined by a corridor with the MBTL.

2. LAUNCHER

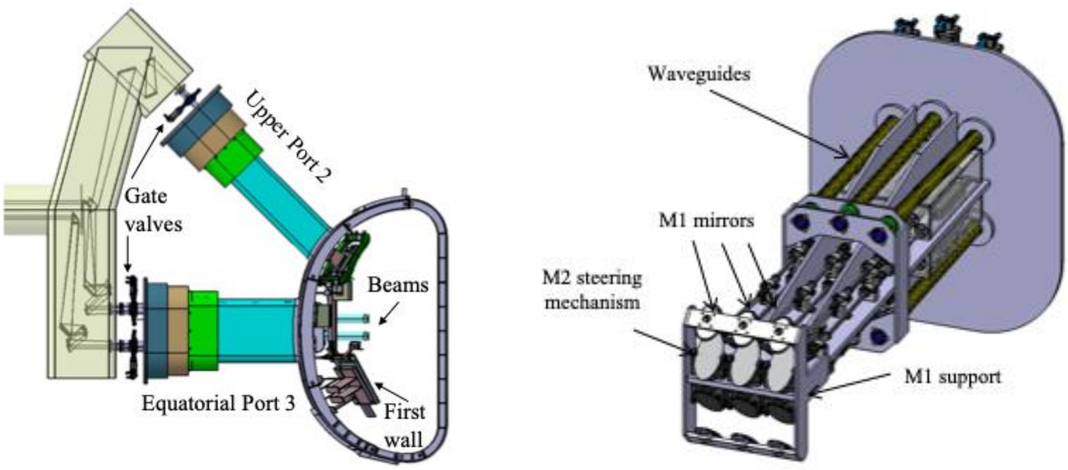

FIG. 2. Left: Side view of DTT sector with Upper and Equatorial ports dedicated to ECRH antennas. Right: Equatorial antenna with waveguides with front view of the top and bottom modules of the mirrors.

A total of 32 launchers will be installed to deliver the EC power required to heat the DTT plasma. For each of the four sectors dedicated to ECRH, the eight beam lines of each cluster have been arranged in two different antennas, six in the equatorial port and two in the upper ports (Fig. 2 Left). All lines are nearly identical and can be independently controlled, providing both modularity and operational flexibility. Each launcher is composed of a cooled corrugated waveguide and two metallic mirrors arranged in a dogleg configuration. The optical design of the mirrors, based on the Gaussian beam optics, adopts a front-steering approach: the first mirror (M1) is fixed and refocuses the beam coming from the TL, while the second mirror (M2), facing the plasma, is flat and steerable in both poloidal and toroidal directions, to accurately aim the beam inside the vessel (Fig. 2 Right). The antennas conceptual design is described in [5].

Both mirrors require active cooling to sustain the thermal load arising from ohmic losses of the 1 MW incident beam as well as from plasma and microwave stray radiation during the 100 seconds of pulse. Additionally, the strong magnetic field surronding the mirrors and their supports must be properly considered, not only during normal tokamak operation but also in presence of major disruptions and vertical displacement events. In these conditions, the induced electromagnetic currents generate structural loads on the antenna, resulting in forces and torques. In particular, in the front part of the structure (where static magnetic field exceeds 4 T) these loads cause deformations and stresses above acceptable limits, especially on the fixed mirrors M1 in copper alloy. Antenna design is under optimization to reduce the structure deformation by minimising horizontal plate extension in the high-B field zone and increasing stiffness, with cage-type structure, avoiding current loops. The design of the launcher mirrors has been improved to reduce electromagnetic forces and thermal stresses and the additive manufacturing technique has been chosen for their realization [6]. The cooling layout is based on a spiral channel for both M1 and M2. Current activities focus on the investigation of alternative materials to CuCrZr with the goal of minimizing induced currents, as well as analyzing different cooling configurations to keep the thermal deformation low. An M2 prototype mirror has been produced in AISI316 with a cooling layer composed by Triple Periodic Minimal Surfaces (TPMS) that forces the cooling fluid to follow a complex path, assuring a low-pressure drop and an enhanced heat transfer coefficient. The mirror has been additively manufactured to test feasibility and limits of manufacturing of TPMS, in particular to investigate the de-powdering process. In addition, thermomechanical simulations indicate critical behavior, particularly at the cooling outlet. This leads to a preference for adopting a spiral-based solution, which would simplify manufacturing and facilitate the monitoring of the water cooling. The cooling strategy is therefore based on the variable depth complementary spiral concept in which the channel depth is adapted to incoming heat load. Thermomechanical simulations assessing the trade-off between cooling efficiency and induced currents reveal critical limitations for AISI316, whereas Inconel 718 and a composite of AISI316 with a copper insert exhibit cooling performance nearly comparable to that of TPMS structures. Additive manufacturing has been demonstrated as feasible for Inconel 718, while other fabrication techniques are under consideration for the composite solution. [7]. Two options for the M2 driving mechanism are under development. The first approach relies on in-vessel under vacuum piezoelectric actuators, combined with flexible joints [8]. Recently, flexible elements for mirror support and drive transmission have been identified, such as cartwheel pivots made of titanium grade 5 and a remote center of motion mechanism for back support of the mirror. The maximum actuator force, in the range of 50–100 N, imposes a limitation on the electromagnetic forces that can be applied to M2, that requires adequate bulk material to steer power. To mitigate this issue, a second option adopts a more standard approach, implementing electrohydraulic linear actuators, at atmospheric pressure, combined with rods, bearing and universal joints for support and motion transmission. Realization of a prototype for each option is mandatory before finalizing the choice, in order to compare feasibility and potential improvements in dynamic performance, ensuring a lifetime that is compatible with the DTT operational schedule.

First evaluations to assess the possible residual EC radiation, not absorbed by the plasma and hitting the in-vessel walls, have been carried out with the quasi-optical raytracing code GRAY [9]. No critical issues have been found operating in the flat-top phase of the full-power, full-field plasma scenario, provided the coupling with Ordinary Mode (OM) is optimal. The EC power coupled to OM is completely absorbed by the plasma at the first harmonic resonance, for the whole interval of launching angles allowed by engineering constraints. However, non-optimal polarization control, with a fraction of the order of few percent of the injected power coupled to the eXtraordinary Mode (XM), might result in high level of residual EC radiation at in-vessel components. XM waves entering the plasma from the low field side encounter a cut-off very close to the plasma edge and the injected beam is back reflected to the first wall, with a path from the launching mirror to the first wall possibly shorter than 1 m. When launching from the Upper Launcher with low toroidal angle, the footprint of the reflected beam at the first wall can be, in extreme cases, smaller than ~30 cm^2. Under such conditions, a 1% coupling to XM at the plasma boundary might already result in a RF power density at the first wall larger than 3 MW/m^2. Such RF power density value should be marginally tolerable by the first wall, but care should be taken to avoid a direct illumination of the diagnostics ports. Additional studies are ongoing to quantify the intensity of diffuse radiation, however strong requirements on EC beam polarization control appear unavoidable to assure safe machine operations.

3. TRANSMISSION LINE

The TL design relies on fully quasi-optical propagation of multiple Gaussian beams. For the most part, the TL exploits the multiple beam (MB) option with eight beams sharing oversized focusing and planar mirrors [10], in a confocal arrangement to compensate for the distortions caused by off-axis reflections, applying the same concept used in W7-X TL but propagating under vacuum to significantly lower the risk of arcing. Standard single beam (SB) sections connect the MB section with the gyrotron and with the antennae, at the beginning and at the end of the TL, respectively. In particular, eight small mirrors combine the beams coming from the gyrotron into a bundle of parallel beams towards the first MB mirror, while at the end of MB section other eight small mirrors split the eight parallel beams towards the two antennae located in the equatorial and upper ports. At least 80 mirrors per cluster are required to cover the ~100 m that each of the 8 beams must travel from the source to the plasma. The TL layout has been analyzed using electromagnetic tools under ideal conditions, perfect alignment and undeformed mirror surfaces, to evaluate the target transmission efficiency of over 90% [11]. The performance includes the contribution by ohmic losses at the reflective surface of the mirrors and spillover fraction, both unavoidable due to the finite electrical conductivity of the materials and the finite size of the mirrors. Ohmic losses, even if representing a small fraction of the total power, require active cooling of the components. Several solutions were studied with spirals [12,13] or TPMS [14]. A maximum total deformation of about 30 µm was obtained for SB mirrors, while TPMS was adopted for the combiner/splitter mirrors, which are the mirrors with the higher load, obtaining maximum total deformation of about 60 µm. Two prototypes in CuCrZr were therefore realized in additive manufacturing using the laser powder bed fusion technology. The first with spiral channel completed the post-printing machining and is presently installed in the Connection Line (CL) box, designed for high-power tests of prototypes, as discussed in sec. 4. The second prototype was manufactured with the TPMS structure to test possible depowdering issues due to the very tight structure of the cooling. A solution with simpler spiral channel was also studied, with results comparable to other SB mirrors, as shown in Fig. 3.

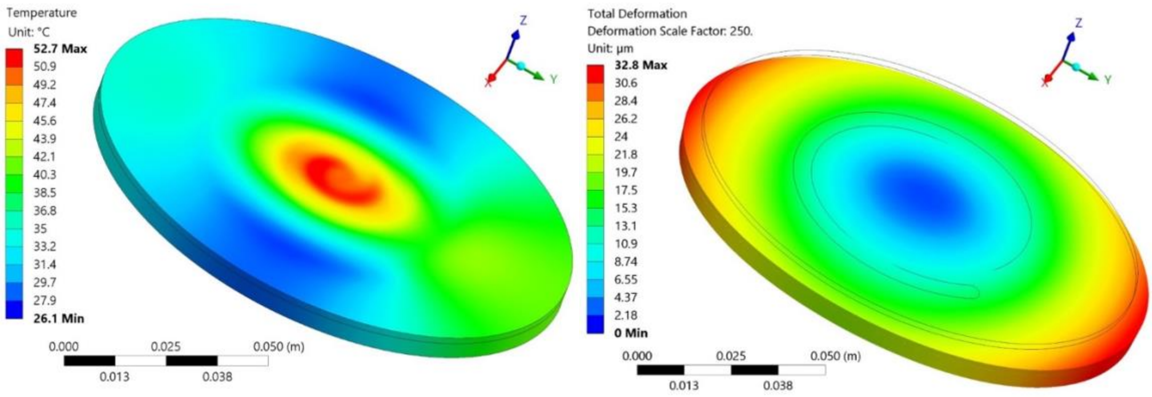

FIG. 3. Left: temperature field of combiner mirror with a spiral channel cooling solution. Right: corresponding total deformation.

For this reason, the solution of spiral channel will be used in all mirrors, while TPMS remains an option for the polarizer mirrors. Each DTT beam line incorporates a universal polarizer system (P1–P2) for matching the injected wave polarization to the plasma. An analytical modeling, design, and validation of a sinusoidal grating elliptical polarizer has been developed [15]. The program computes the polarization properties for arbitrary corrugation profiles without requiring 3D simulations, achieving validation against HFSS commercial code with an error of about 0.5%. The method enables optimization of corrugation depth, full control of output polarization with combined polarizers, and provides a reliable tool for polarizer design and real-time control of the polarization of the injected wave in the plasma. The tool allows also for the estimation of the enhanced ohmic losses linked to the corrugation, with heat load up to 32 times higher than standard SB mirrors. It thus requires a very efficient cooling, like the TPMS, but also a revision of the optical layout to make the heat load on these mirrors as low as possible. Finally, a cooling solution with multi-spiral channels in parallel was analyzed also for MB mirrors, with resulting maximum deformation between 60 and 90 µm, depending on the kind of mirrors. An option for the cooling of MB mirrors with a single spiral channel is presently under study to simplify design, manufacturing, and water monitoring. This configuration has been studied taking into account possible lightening and strengthening of the structure, obtainable by additive manufacturing, with the target of procuring a full-scale prototype in 2026. The expected effect of non-idealities on TL performances due to mirrors' deformation and misalignments arising from installation errors or accidental loads is to increase the stray radiation in the TL enclosure, especially in the splitter section [11]. The possibility to recover the alignment for limiting these effects was also investigated. The simplest option is to fit two MB mirrors with two vacuum compatible actuators, using two bi-axial sensors for monitoring misalignments, one on the last MB mirror and the other at the centre of the octagon of the splitters. The two actuated MB mirrors were chosen with Montecarlo simulations with the goal to minimize the average misalignment along the TL. In this way, it will be possible to recover the misalignments also between two plasma pulses, without breaking the vacuum in the TL enclosure.

4. GYROTRON & POWER SUPPLY

The source specifications have exploited the ITER gyrotron project which led to a joint open and international procurement with the F4E, ultimately choosing Thales as the gyrotron supplier. This new approach provided the opportunity to continuously coordinate priorities for both projects assuring strong synergy in the contract's execution. Each DTT gyrotron delivers 1 MW of power at 170 GHz for 100 s, with an efficiency larger than 40%. The first DTT gyrotron has been manufactured and tested at the FALCON facility (Fig. 4 Left), confirming compliance with the frequency, pulse length, output power and efficiency requirements. Fig. 4 right shows for shot #14501 the time evolution of the power measured at the Matching Optics Unit during a 100 s pulse test, with a stability below 5%, having an electron current beam of 48 A on average. The operating parameters were optimized to reach the maximum performance of the gyrotron and were set for these tests with a cavity magnetic field B_{cav} = 6.69 T, a beam voltage of V_{acc} =79.5 kV and a body voltage V_{body} = 24.5 kV. On this basis, the contract for the production of the next 15 gyrotrons has been initiated, ensuring completion of the supply required for the first phase of DTT [16].

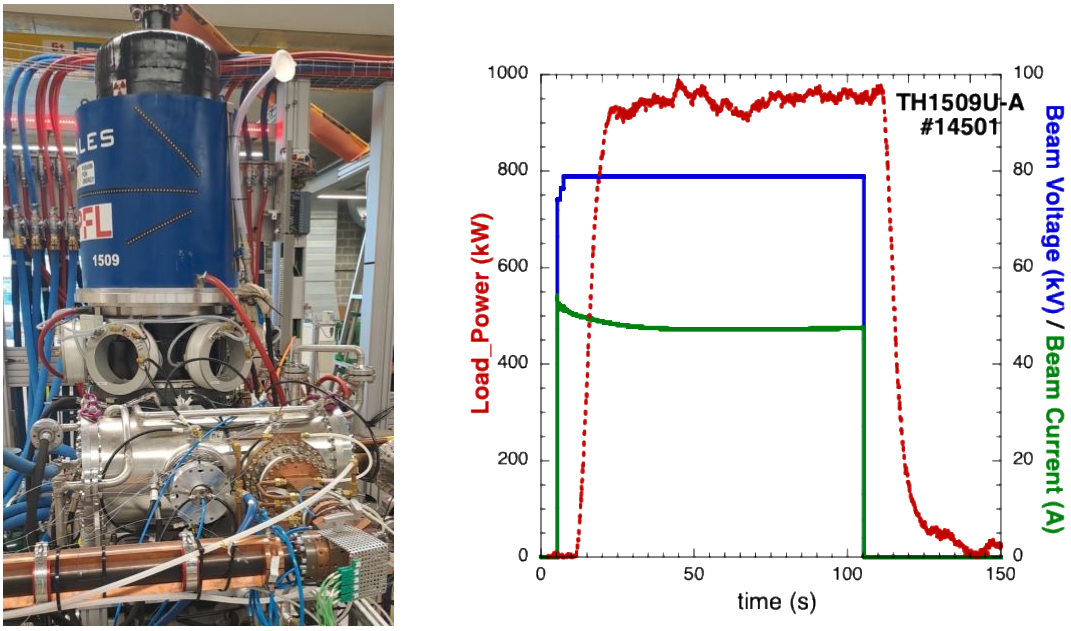

FIG. 4. Left: First DTT gyrotron at FALCON test facility under commissioning. Right: Time evolution of gyrotron power measured after the Matching Optics Unit (red) and related beam voltage (blue) and current (green) for the pulse #14501.

Each pair of gyrotrons is powered by a single High Voltage Power Supply (HVPS) set, composed of: a Main Power Supply (MPS) that feeds both gyrotrons in parallel; two Body Power Supplies (BPS), each individually dedicated to a single gyrotron; two Filament Power Supplies (FPS) for the filament heaters. The MPS is rated at -60 kVdc and 110 A (2 × 55 A), negatively polarizing the cathode relative to the grounded collector to supply the primary power to the electron beam. Meanwhile the BPS operates at 30 kVdc and 100 mA, positively polarizing the body electrode. The FPS supplies with DC current the heater of the electron beam emitter to keep it at high temperature. This requires high voltage insulation of the output terminals with respect to ground, since they are at the MPS negative potential. The HVPS system is designed with fast output voltage dynamics, including ramp-up and ramp-down times lower than 50 µs / 30 µs for the MPS / BPS respectively to minimize the excitation of competing RF modes during voltage increases. A stringent settling time of under 20 µs ensures a stable flat-top voltage, enabling effective modulation at frequencies of up to 5 kHz [17]. The conceptual design, covering the power supply of the cathodes, body electrodes, and filament heaters, has been completed, and the technical specifications have been defined for the procurement of the first eight sets.

A short evacuated Connection Line (CL), designed to route the gyrotron output to the RF load in free space propagation and accommodate different mirrors, has been realized for use at the FALCON. This mirror, fabricated by additive manufacturing in CuCrZr alloy, is water-cooled, mounted on a dedicated support, and adjustable along

two tilt axes. The mirror assembly is housed within a vacuum vessel equipped with an external cooling jacket and two lateral arms to preserve the evacuated region along the beam trajectory. The vessel support provides fine positioning capability along the x, y, and z directions. The CL has been conceived to facilitate gyrotron output beam characterization as well as the testing of alternative mirror technologies for R&D purposes. Its optical and mechanical design ensures compatibility with both the FALCON facility and the DTT ECRH building, where it will also serve for gyrotron commissioning. The CL was fully assembled at CNR-ISTP (Fig. 5 left). Integrity of the cooling jacket was confirmed through water flow testing, and both leak detection and vacuum qualification were successfully completed, achieving a pressure of 1.2×10^{-2} mbar [16].
Additionally, the procurement of four RF loads for the first two clusters is currently in progress and scheduled for completion in 2026. Each cluster will be equipped with two RF loads: one dedicated to daily commissioning at the combining mirror (also used for gyrotron commissioning), and another located at the end of the MBTL for mirror conditioning, diagnostics calibration, alignment, and polarization verification. The FAT of the first load has been successfully completed at Curti Costruzioni Meccaniche–LT Calcoli (Fig. 5, right), and the load is now being delivered to FALCON for the SAT using the DTT gyrotron.

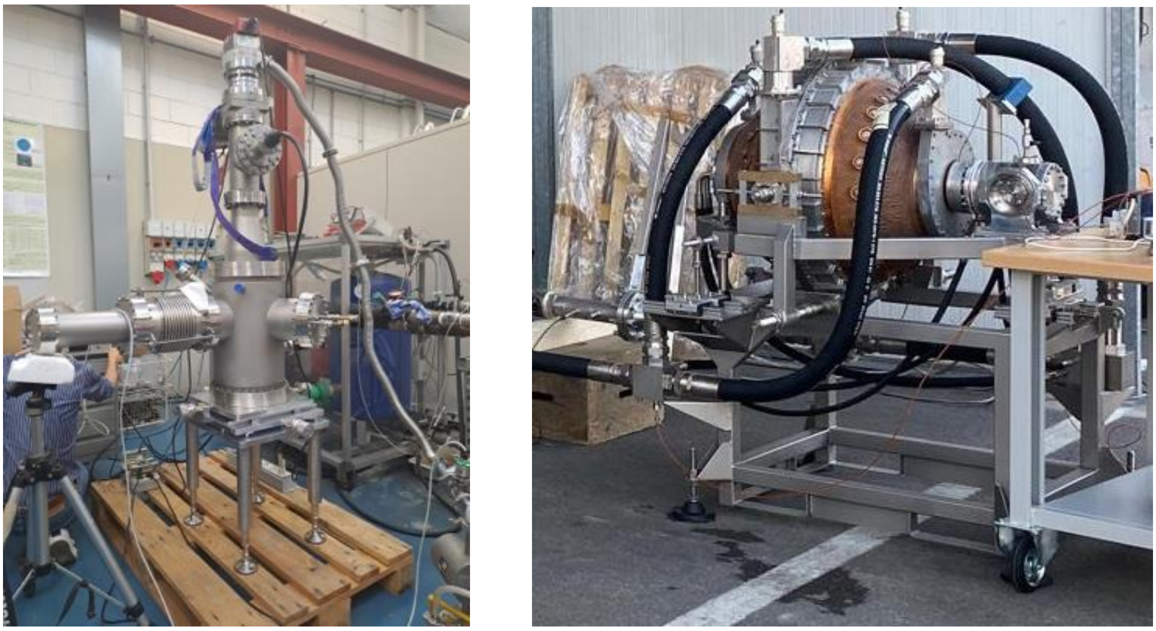

FIG. 5. Left: Connection Line at ISTP-CNR laboratory. Right: RF Load at factory acceptance test.

5. CONTROL SYSTEM

The architecture of the ECRH control system is designed to ensure maximum flexibility in the use of the system during the DTT plasma operations while maintaining an optimized power availability. It is organized as a network of Plant Systems Units (PSUs), acting as intermediaries between the central COntrol & Data Acquisition System (CODAS), the Plasma Control System (PCS) and the individual plant components. Their role is to standardize interactions, by setting aside low-level implementation details and providing a uniform control interface across all components. All the PSUs are coordinated by an ECRH plant supervisor, located in the CODAS/PCS. The supervisor acts both as a scheduler and conversion layer, translating high-level plasma physics requests (e.g., power level, deposition area) into engineering-level commands and reference signals for the PSUs. For testing and maintenance activities not scheduled by CODAS, an asynchronous supervisor is also foreseen as responsible for the operation of a single pair of gyrotrons, fed by the same HVPS set, to allow high availability of the ECRH system as required in DTT. Each PSU consists of three core elements to implement and manage controls and protections functions: the Slow Control Unit (SCU), Fast Control Unit (FCU), and Fast Alarm & Safety Unit (FA&SU).
The SCU is based on a Programmable Logic Controller (PLC) and is dedicated to slow protections and low-frequency communications (≤ 1 kHz). It receives commands and configuration parameters from the CODAS and returns status information, as well as low-frequency data and parameters.
The FCU is responsible for low-level control and real-time control of individual Plant Units, in particular it produces the real time references for the HVPS set.

The FASU is implemented with dedicated hardware solutions for arc detection and for generating fast interlock signals to protect the gyrotrons and other relevant components of the ECRH system.
Each PSU has been adapted to the specific plant subsystem to be controlled. The Double Gyrotron Control Unit (DGCU) is responsible for managing and controlling a pair of gyrotrons. Its functions include operating the fast power supplies (MHVPS, BPS and filament heater) and controlling the auxiliaries (SCM system, vertical & radial sweeping coils and ion pumps). It also provides general monitoring of gyrotron including temperature of collector and shaft, oil temperature and water parameters (temperature, pressure, and flow). The Transmission Line Control Unit (TLCU) manages and monitors all Plant Units (PUs) that enable the transmission of RF power from the gyrotron building to the tokamak hall. It also governs the appropriate routing of power to the RF loads during testing and conditioning phases, supervises the vacuum conditions along the TL, ensures correct optical alignment of the mirrors, control the temperature of the TL components and detect arcs. The Launcher Control Unit (LCU) has the primary function of directing microwaves into the plasma with optimal polarization providing synchronized control of both polarizers and launchers. Similar to the DGCU, it manages paired launchers. For each launcher, LCU monitors mirrors temperatures and implements closed-loop control of low-level actuators (plant units) to adjust the orientation of the launching mirrors and the polarizers. It also manages arc detection and stray radiation measurements. The LoadCU is responsible for the management, monitoring and control of the activities on the RF Load. A dedicated slow control unit monitors the RF power by bolometric measurement that uses water flow and temperature. In addition, 24 temperature sensors are installed on the load itself to track operating conditions and ensure safety.

6. CONCLUSIONS

The development of the ECRH system marks a decisive step toward addressing the main heating system of the future DTT tokamak. Designed to combine high performance with operational flexibility, the system integrates proven and consolidated technologies with the most advanced available today, including multi-beam quasi-optical transmission, additive manufacturing of complex components, innovative cooling strategies, and robust high-precision actuation mechanisms. The coordinated progress of all subsystems — gyrotrons, transmission lines, launchers, control architecture, and RF loads — reflects a strongly integrated approach that is essential to ensure the ambitious performance targets of DTT within its demanding timeline. Looking ahead, the knowledge being gained through the development of the DTT ECRH system will also play a key role in shaping the design and operation of microwave systems for future fusion reactors, ultimately contributing to the realization of DEMO.

ACKNOWLEDGEMENTS

This work is carried out in the frame of the DTT activity. The authors are very grateful to all the colleagues involved in the DTT project for their precious contributions.

REFERENCES

[1] ROMANELLI F. et al., Nucl. Fusion, **64** (2025) 112015.
[2] GARAVAGLIA S. et al., J. Vac. Sci. Technol. B, **41** (2023) 044201.
[3] GARAVAGLIA S. et al., Fusion Eng. Des., **168** (2019) 112678.
[4] GRANUCCI G. et al., Nucl. Fusion, **64** (2024) 126036.
[5] FANALE F. et al., Fusion Eng. Des., **192** (2023) 113797.
[6] PEPATO A. et al., Fusion Eng. Des., **219** (2025) 115238.
[7] PAGLIARO A. et al., Submitted to Fusion Eng. Des.
[8] BUSI D. et al., Fusion Eng. Des., **180** (2022) 113196.
[9] FARINA D., Fusion Sci. Technol., **52** (2007) 154.
[10] BRUSCHI A. et al., Fusion Eng. Des., **194** (2023) 113727.
[11] MORO A. et al., Fusion Eng. Des., **202** (2024) 114391.
[12] SALVITTI A. et al., Fusion Eng. Des., **201**, (2024) 114228.
[13] SALVITTI A. et al., Fusion Eng. Des., **216**, (2025) 115088.
[14] GAJETTI E. et al., IEEE T PLASMA SCI **52**(9), (2024) 3765-3771.
[15] BERTOLAMI S. et al., Submitted to Fusion Eng. Des.
[16] GARAVAGLIA S. et al., Submitted to Fusion Eng. Des.
[17] RECCHIA M., IEEE Tra. Plasma Sci., **52** (2024) 4069-4074.